JACS
JOURNAL OF THE AMERICAN CHEMICAL SOCIETY

Communication

pubs.acs.org/JACS

High-Precision Tracking with Non-blinking Quantum Dots Resolves Nanoscale Vertical Displacement

Kyle Marchuk, Yijun Guo, Wei Sun, Javier Vela, and Ning Fang*

Ames Laboratory, U.S. Department of Energy, and Department of Chemistry, Iowa State University, Ames, Iowa 50011, United States

Supporting Information

ABSTRACT: Novel non-blinking quantum dots (NBQDs) were utilized in three-dimensional super-localization, high-precision tracking applications under an automated scanning-angle total internal reflection fluorescence microscope (SA-TIRFM). NBQDs were randomly attached to stationary microtubules along the radial axis under gliding assay conditions. By automatically scanning through a wide range of incident angles with different evanescent-field layer thicknesses, the fluorescence intensity decay curves were obtained. Fit with theoretical decay functions, the absolute vertical positions were determined with sub-10-nm localization precision. The emission intensity profile of the NBQDs attached to kinesin-propelled microtubules was used to resolve the self-rotation of gliding microtubules within a small vertical distance of ~50 nm. We demonstrate the applicability of NBQDs in high-precision fluorescence imaging experiments.

Tracking single-molecule and nanoparticle probes with a precision of sub-nanometer to a few tens of nanometers is crucial for elucidating nanoscale structures and movements in biological systems. Semiconductor quantum dots (QDs) have intrinsic fluorescence properties that hold advantage over traditional organic fluorophores such as broad absorption and narrow size-tunable emission spectra[1,2] and increased photostability;[3] however, the use of QDs in high-precision single-particle tracking (SPT) applications has been greatly limited by their intrinsic trait of single-particle fluorescence intermittency, commonly referred to as "blinking". While mild reducing agents or electron-donating environments can help suppress this trait,[4,5] these methods are not always applicable. These reagents can present problems for biological systems by causing interruptions to disulfide linkages and other redox-susceptible groups in biomolecules, or simply, methods such as these may not suppress intermittency enough to be useful in high-precision SPT experiments.

The introduction of a new type of core/shell semiconductor QDs[6−8] satisfies many of the needs for continuous-emission single-fluorophore experiments. These QDs are referred to as non-blinking quantum dots (NBQDs) for their statistical supremacy in fluorescence intermittency behavior compared to conventional QDs. However, even with all the hype around NBQDs, to the best of our knowledge, there has not been any study that realizes the full potential of NBQDs for three-dimensional (3D) high-precision dynamic tracking.[9]

While super-localization in the horizontal (x−y) plane is now considered a routine procedure, superlocalization in the axial (z) direction remains challenging and requires special techniques, including invoking optical astigmatism,[10] biplane imaging,[11,12] temporal focusing,[13] or using a double-helix point spread function.[14] In the present study, we employed a fully automated prism-type scanning-angle total internal reflection fluorescence microscope (SA-TIRFM)[15,16] in combination with NBQDs for 3D dynamic tracking near the total internal reflection (TIR) interface with a sub-10-nm axial localization precision.

The use of TIR geometry holds many advantages in single-particle localization and tracking experiments.[17] The generation of an exponentially decaying evanescent field (EF) at the surface of TIR allows for significant background reduction, while the depth of the EF can be adjusted with control of the incident illumination angle. Our SA-TIRFM uses an in-house computer program that can accurately determine the ideal illumination area under the objective and reliably reproduce the position for a wide range of angles.[15,16] Combined with the continuous fluorescent emission from the NBQDs, the SA-TIRFM can locate and track events taking place within the EF with exceptionally high precision. The use of NBQDs is necessary to avoid erratic fluorescent emission curves due to conventional QDs' tendency to blink during system calibration and data acquisition.

The high axial localization precision of our imaging system was utilized to determine the absolute vertical positions of NBQDs attached to stationary microtubules and resolve the rotational motion of gliding microtubules, which takes place within a vertical distance of ~50 nm near the substrate surface. Motor proteins, such as kinesin, are essential to cellular functions by transporting intracellular cargo throughout the cell. This ability illuminates the great potential of motor proteins to serve in engineered transport systems as components in nanomachines that sort and shuttle cargo to designated locations. It has been found that by fixing kinesin to a surface followed by introducing solutions of microtubules and adenosine-5′-triphosphate (ATP), the microtubules will be propelled laterally.[18−25] The number of protofilaments composing the microtubule determines the particular motion the microtubule undertakes as it is propelled by kinesin. If a microtubule is composed of protofilament count differing from 13, the microtubule rotates around its longitudinal axis due to the stepwise motion of kinesin.[18] Using conventional QDs in

Received: February 9, 2012
Published: March 29, 2012

dx.doi.org/10.1021/ja301332t | J. Am. Chem. Soc. 2012, 134, 6108−6111

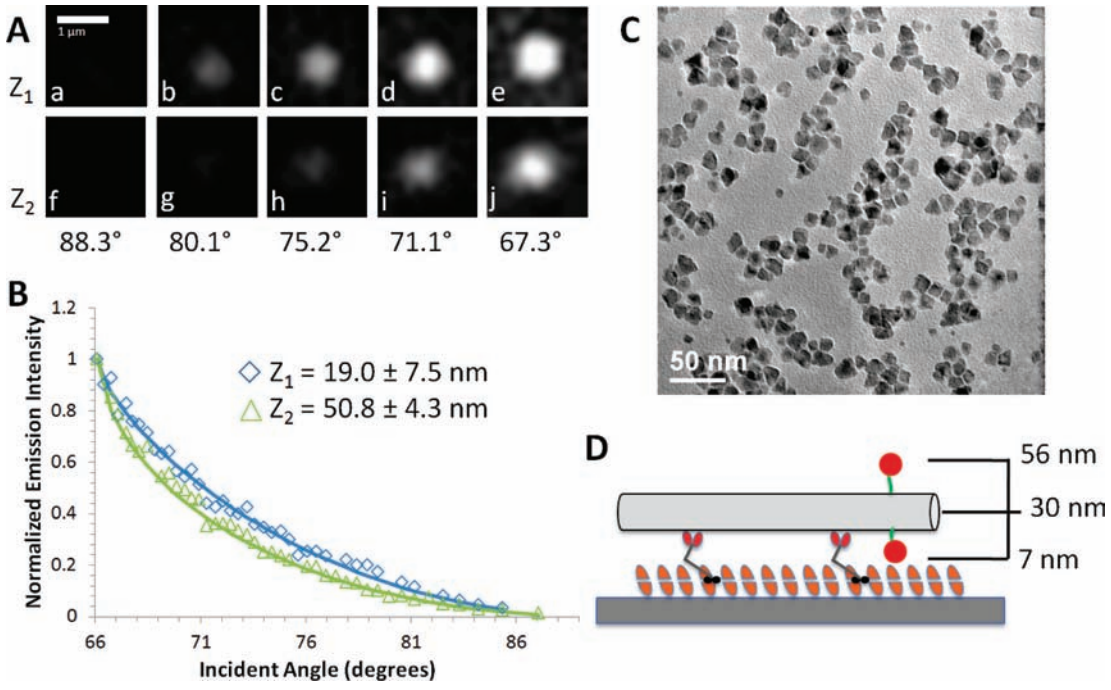

Figure 1. (A) Image set of NBQDs located at different axial positions on stationary microtubules: (a–e) those for z_1 at axial distance 19.0 ± 7.5 nm and (f–j) those for z_2 at axial distance 50.8 ± 4.3 nm. (B) Fluorescence intensity decay curves for particles z_1 and z_2. (C) TEM image of NBQDs CdSe(4.7 nm)-17CdS. (D) Cartoon representing important distances of the rotational-microtubule NBQD system (not drawn to scale).

fluorescence interference contrast (FLIC) microscopy[24] or plasmonic gold nanorods in single particle orientation and rotational tracking (SPORT) under a differential interference contrast (DIC) microscope,[15] the detection of the gliding self-rotation was successfully demonstrated. Herein, we present a novel approach to resolve the rotational motion by precisely following the vertical positions of the NBQDs attached to the self-rotating microtubules.

Thick-shell NBQDs with a 4.7-nm-diameter CdSe core surrounded by 17 atomic monolayers (MLs) of CdS (CdSe/17CdS) were synthesized following our recently published approach that gives an improved synthetic reliability and reproducibility compared to previous methods.[26] Comprehensive statistical analyses of the fluorescence intermittency for the NBQDs, thin-shell quantum dots (TSQDs), and commercial QDs (EviTag T2) were performed for a large sample size of individual particles (see Supporting Information (SI), Supplementary Table 1 for details). Without modification or a blinking-suppressing environment, the NBQDs easily surpass the commercial QDs with regard to fluorescence intermittency. These statistics make the absolute positioning and 3D dynamic tracking of NBQDs possible.

Axial localization was accomplished by attaching the NBQDs through the biotin–neutravidin interaction under gliding assay conditions in quartz microscope slide chambers. The microtubules were held static by withholding the final ATP-rich gliding assay solution (see SI for details). The incident angle of the excitation laser was varied from the large angle of 88.3° to the critical angle of 67.3° in increments of ∼0.25°, which expanded the EF deeper into the sample. Figure 1A shows the increase in fluorescence signal for two NBQDs attached to microtubules at different axial positions as the incident angle was varied. It can be easily seen that the relative vertical distances of the NBQDs labeled as 1 and 2 have a relationship of $z_1 < z_2$. Their *absolute* axial distances can be determined to be 19.0 ± 7.5 and 50.8 ± 4.3 nm, respectively, by nonlinear least-squares (NLLS) fitting[15] of the intensity curves shown in Figure 1B. These measurements fall within the expected range of vertical distances dictated by the geometrical constraints of the system (Figure 1D), which include the size of the microtubule, length of kinesin, biotin–neutravidin interaction, and diameter of the NBQD.

A complete explanation of the error analysis used in the NLLS fitting can be found in the SI, and a thorough uncertainty study can be found in our previous work.[15] Briefly, a χ^2 test was performed on the experimental and theoretical fluorescence values for each angle. A confidence interval for the calculated z was then determined using F_χ statistics for the appropriate parameters and degrees of freedom. It should be emphasized that the high localization precision was realized with the ability of our instrument to find and replicate the optimal incident illumination light angles and the consistency of the NBQDs to stay in the fluorescent emission state for prolonged periods of time.

The NBQDs are ideal probes not only for axial localization in static systems but also for tracking 3D position changes in dynamic systems. The absolute position cannot be determined for dynamic systems using SA-TIRF due to the time needed to image multiple angles; however, our system allows for the relative axial changes to be idealized. Microtubules composed of 13 protofilaments do not rotate while moving laterally across a kinesin-coated surface. Therefore, the expected trace produced by a NBQD attached to a gliding microtubule would be a consistent signal as the microtubule travels along at the same depth in the EF. Figure 2 displays a trace produced by a NBQD attached to a microtubule propelled by kinesin.

As can be seen, the NBQD did not blink once during the entire acquisition, which allowed the determination of this non-rotating microtubule (SI, Movie 1). Supplementary Figure 1 portrays a comparison between NBQDs and TSQDs under

dx.doi.org/10.1021/ja301332t | J. Am. Chem. Soc. 2012, 134, 6108–6111

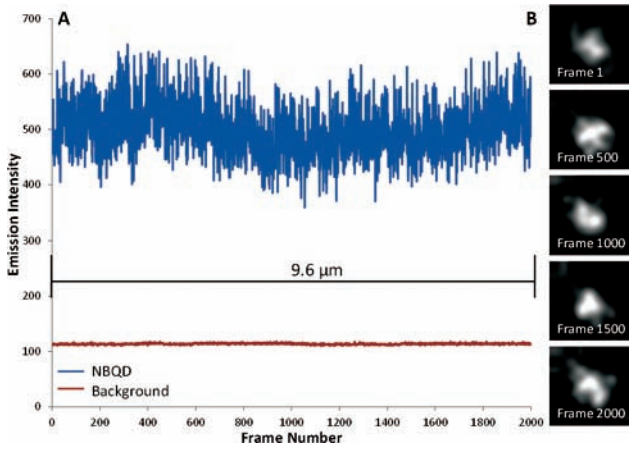

Figure 2. (A) Trace of NBQD attached to kinesin-propelled microtubule in gliding assay (50 ms exposure time). (B) Images of NBQD every 500 frames throughout the trace of (A).

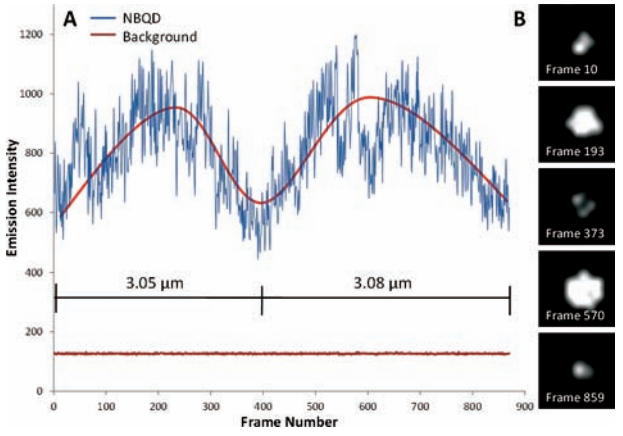

Figure 3. (A) Trace of NBQD attached to rotating microtubule followed for two full periods (50 ms exposure time). (B) Images of NBQD at frames corresponding to minima and maxima of (A).

gliding assay conditions both moving (with ATP) and stationary (without ATP). The protofilament count of the moving microtubule to which the TSQD is attached is lost in the ambiguity of the emission profile. It is impossible to discern whether the fluctuations in emission intensity are due completely to the fluorescence intermittency or whether there is a change in the axial distance of the TSQD as the microtubule glides across the surface. It should be noted that an oxygen scavenging system (described in SI) is present for all examples of microtubule motion but is not present for stationary microtubules.

The self-induced longitudinal rotation of non-13-protofilament microtubules with attached NBQDs is confined to a z-depth of ∼50 nm. It is important to choose an incident angle that will most readily reveal this minimal axial translation. An advantage of the automated SA-TIRFM is the ability to easily select an ideal angle for a given set of experiments and reproduce it reliably. The depth $d(\theta)$ of the EF propagating from the surface of TIR is directly related to the angle of incident light, which corresponds to the fluorescence intensity decay at various axial distances (z). Thus, a larger angle equates to a thinner EF, which produces a greater relative change in fluorescence intensity as the axial position of the fluorophore changes. This relationship can be visualized in Supplementary Figure 2.

The ideal angle for tracking the rotation of NBQDs attached to microtubules maximizes the change of fluorescence intensity as the NBQD moves toward and away from the TIR surface, while keeping the minimum emission intensity above the background noise. This aspect is also limited by other practical elements of the experiment such as the quantum efficiency of the probe and the intensity of the excitation source.

With the proper angle chosen, a vast amount of information was readily discernible from the intensity profiles produced in the NBQD traces. Figure 3 shows an example trace of a NBQD attached to a rotating microtubule followed for two full periods (SI, Movie 2). It is easy to observe the maximum and minimum intensities as the microtubule travels laterally across the surface. The fluorescence intensity trace seen in Figure 3A was recorded using an incident angle of 80.1°, which produces an EF depth of near 77 nm. The relative change in axial distance Δz was calculated[27] to be 49.5 nm, which translates to the axial distance traveled by the NBQD during microtubule rotation. This value aligns well with the estimated geometrical constraints previously mentioned. Using a particle tracking plugin within the open-source program ImageJ, we tracked the lateral distance traveled during the periods of rotation. The distances were measured to be ∼3.1 μm for both rotations. This corresponds to the super-twist length of a microtubule composed of 12 protofilaments.[18]

A second microtubule trace was analyzed, which can be seen in Supplementary Figure 3A. For this recording a smaller incident light angle of 75.6° was used, which produced an EF depth of 90 nm. The rotation curve is noticeably shallower than the one seen in Figure 2. Though this makes the determination of the fluorescence minimum slightly more difficult, the axial rotation distance of 45.6 nm was calculated, and the lateral distance traveled was measured at 5.4 and 5.7 μm from the two rotations. These lateral distances correspond to a 14-protofilament microtubule.[18]

In summary, novel QDs with suppressed fluorescence intermittency were used in 3D super-localization and dynamic tracking experiments to achieve exceptionally high precision. The combination of the fully automated SA-TIRFM and NBQDs enabled us to find the absolute vertical positions of NBQDs attached along the rotational axis of stationary microtubules. The ability to easily tune the incident illumination angle and the stable fluorescence signal of NBQDs allowed us to discern the self-rotation of kinesin-driven microtubules taking place within a limited axial width. Looking forward, as the understanding of fluorescence intermittency increases, QDs will continue to become more versatile in their applications. Already, prolate nanocrystals have been published that continuously fluoresce by utilizing a gradated core/shell synthetic procedure.[7] As this and other techniques produce smaller and brighter "non-blinking" semiconductor probes with reduced cytotoxicity, opportunities will arise in such applications as intracellular multi-color single-molecule tracking, observing signal transduction pathways, and understanding membrane processes such as endocytosis, exocytosis, and the formation and function of membrane micro- and nanodomains.

dx.doi.org/10.1021/ja301332t | J. Am. Chem. Soc. 2012, 134, 6108−6111

■ ASSOCIATED CONTENT

Supporting Information

Materials and methods, supplementary table and figures, and three movies in .avi format. This material is available free of charge via the Internet at http://pubs.acs.org.

■ AUTHOR INFORMATION

Corresponding Author

nfang@iastate.edu

Notes

The authors declare no competing financial interest.

■ ACKNOWLEDGMENTS

This work was supported by the U.S. Department of Energy, Office of Basic Energy Sciences, Division of Chemical Sciences, Geosciences, and Biosciences through the Ames Laboratory. The Ames Laboratory is operated for the U.S. Department of Energy by Iowa State University under Contract DE-AC02-07CH11358. Y.G. was also supported in part by Plant Science Institute at Iowa State University.

■ REFERENCES

(1) Bruchez, M.; Moronne, M.; Gin, P.; Weiss, S.; Alivisatos, A. P. *Science* **1998**, *281*, 2013.
(2) Han, M. Y.; Gao, X. H.; Su, J. Z.; Nie, S. *Nat. Biotechnol.* **2001**, *19*, 631.
(3) Chan, W. C. W.; Nie, S. M. *Science* **1998**, *281*, 2016.
(4) Hohng, S.; Ha, T. *J. Am. Chem. Soc.* **2004**, *126*, 1324.
(5) Fomenko, V.; Nesbitt, D. J. *Nano Lett.* **2008**, *8*, 287.
(6) Chen, Y.; Vela, J.; Htoon, H.; Casson, J. L.; Werder, D. J.; Bussian, D. A.; Klimov, V. I.; Hollingsworth, J. A. *J. Am. Chem. Soc.* **2008**, *130*, 5026.
(7) Wang, X. Y.; Ren, X. F.; Kahen, K.; Hahn, M. A.; Rajeswaran, M.; Maccagnano-Zacher, S.; Silcox, J.; Cragg, G. E.; Efros, A. L.; Krauss, T. D. *Nature* **2009**, *459*, 686.
(8) Mahler, B.; Spinicelli, P.; Buil, S.; Quelin, X.; Hermier, J. P.; Dubertret, B. *Nat. Mater.* **2008**, *7*, 659.
(9) Vela, J.; Htoon, H.; Chen, Y. F.; Park, Y. S.; Ghosh, Y.; Goodwin, P. M.; Werner, J. H.; Wells, N. P.; Casson, J. L.; Hollingsworth, J. A. *J. Biophoton.* **2010**, *3*, 706.
(10) Huang, B.; Wang, W. Q.; Bates, M.; Zhuang, X. W. *Science* **2008**, *319*, 810.
(11) Juette, M. F.; Gould, T. J.; Lessard, M. D.; Mlodzianoski, M. J.; Nagpure, B. S.; Bennett, B. T.; Hess, S. T.; Bewersdorf, J. *Nat. Methods* **2008**, *5*, 527.
(12) Toprak, E.; Balci, H.; Blehm, B. H.; Selvin, P. R. *Nano Lett.* **2007**, *7*, 2043.
(13) Vaziri, A.; Tang, J. Y.; Shroff, H.; Shank, C. V. *Proc. Natl. Acad. Sci. U.S.A.* **2008**, *105*, 20221.
(14) Pavani, S. R. P.; Greengard, A.; Piestun, R. *Appl. Phys. Lett.* **2009**, 95.
(15) Sun, W.; Marchuk, K.; Wang, G. F.; Fang, N. *Anal. Chem.* **2010**, *82*, 2441.
(16) Sun, W.; Xu, A. S.; Marchuk, K.; Wang, G. F.; Fang, N. *JALA* **2011**, *16*, 255.
(17) Axelrod, D. In *Biophysical Tools for Biologists, Vol. 2: In Vivo Techniques*; Correia, J. J., Detrich, H. W., Eds.; Methods in Cell Biology *89*; Academic Press: New York, 2008; p 169.
(18) Ray, S.; Meyhofer, E.; Milligan, R. A.; Howard, J. *J. Cell Biol.* **1993**, *121*, 1083.
(19) Bohm, K. J.; Stracke, R.; Unger, E. *Cell Biol. Int.* **2000**, *24*, 335.
(20) Verma, V.; Hancock, W. O.; Catchmark, J. M. *Biomed. Microdevices* **2009**, *11*, 313.
(21) Huang, Y.-M.; Uppalapati, M.; Hancock, W. O.; Jackson, T. N. *Biomed. Microdevices* **2007**, *9*, 175.
(22) Friedman, D. S.; Vale, R. D. *Nat. Cell Biol.* **1999**, *1*, 293.
(23) Kerssemakers, J.; Howard, J.; Hess, H.; Diez, S. *Proc. Natl. Acad. Sci. U.S.A.* **2006**, *103*, 15812.
(24) Nitzsche, B.; Ruhnow, F.; Diez, S. *Nat. Nanotechnol.* **2008**, *3*, 552.
(25) Ha, J. W.; Sun, W.; Wang, G. F.; Fang, N. *Chem. Commun.* **2011**, *47*, 7743.
(26) Guo, Y.; Marchuk, K.; Sampat, S.; Abraham, R.; Fang, N.; Malko, A. V.; Vela, J. *J. Phys. Chem. C* **2011**, *116*, 2791.
(27) Saffarian, S.; Kirchhausen, T. *Biophys. J.* **2008**, *94*, 2333.